A Theoretical Analysis of Thermic Endfire Interstitial Applicator

Jong-Kweon Park · Hyo-Joon Eom

Abstract

A novel approach for modeling the thermic endfire interstitial applicator is presented. A hypothetical semi-infinite circular cylinder is added in the endfire direction in order to facilitate the theoretical modeling approach. The Fourier transform and mode-matching technique is utilized to obtain a solution in fast-convergent series. Numerical computations for the input impedance are performed to check the validity of the theoretical model.

Key words : thermic endfire interstitial applicator, microwave hyperthermia, mode-matching

Ⅰ. INTRODUCTION

A thermic endfire interstitial applicator has been used for microwave hyperthermia applications and extensively studied [1]~[3]. In [1], a thermic endfire interstitial applicator has been analyzed using the equivalence principle and the reflection coefficient and near field distribution were calculated. The effect of a catheter on the SAR (Specific Absorption Rate) distribution around the coaxial-slot antenna has been also studied in [2] utilizing the moment method. In [3], effective impedance of a circumferential slot on a coaxial transmission line was calculated using the transmission line theory. In the present paper, we intend to model a thermic endfire interstitial applicator by introducing a hypothetical semi-infinite circular cylinder at the end of interstitial applicator. We will use the Fourier transform and mode matching [4] to obtain a rapidly convergent series solution for a thermic endfire interstitial applicator. In the next section, we summarize the final theoretical expressions and their numerical results.

Ⅱ. THEORETICAL AND NUMERICAL RESULTS

Consider the thermic end-fire interstitial applicator as shown in Fig. 1 under TEM mode incidence. For analytic convenience, a semi-infinite circular cylinder is placed in the endfire direction near the end of the interstitial applicator. In regions (I) and (IV), the fields are

$$H_{\phi I}(\rho, z) = \frac{e^{-ik_1 z}}{\eta_1 \rho} + i\omega\varepsilon_1 \frac{2}{\pi}\int_0^{\infty} \frac{1}{k}\tilde{E}_I(\zeta)R'(k\rho)\cos(\zeta z)d\zeta \quad (1)$$

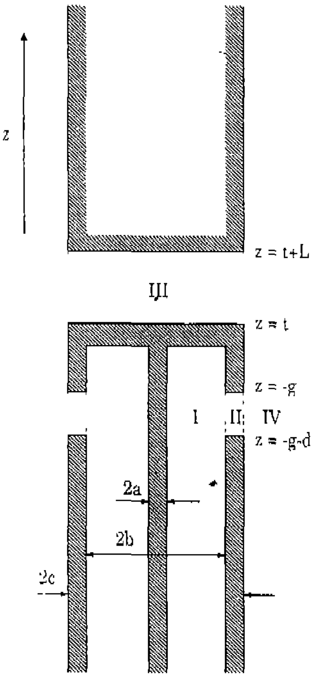

Fig. 1. Geometry of thermic end-fire interstitial applicator.

$$H_{\phi IV}(\rho, z) = \frac{-i\omega\varepsilon_4}{2\pi}\int_{-\infty}^{\infty} \frac{1}{v}\tilde{E}_{IV}(\zeta)H_1^{(1)}(v\rho)e^{-i\zeta z}d\zeta \quad (2)$$

where $R(k\rho) = J_0(k\rho)N_0(ka) - N_0(k\rho)J_0(ka)$, $k = \sqrt{k_1^2 - \zeta^2}$, $\eta_1 = \sqrt{\mu/\varepsilon_1}$, $v = \sqrt{k_3^2 - \zeta^2}$, and $k_i = \omega\sqrt{\mu\varepsilon_0\varepsilon_{ri}}$ for $i = 1,2,3,4$. $R'(.)$ denotes differentiation of $R(.)$ with respect to the argument. $J_n(.)$ and $H_n^{(1)}(.)$ are the n^{th} order Bessel and

Manuscript received March 30, 2001; revised April 25, 2001.

J. K. Park is with the Antenna Technology Center, Radio & Broadcasting Technology Laboratory, Electronics and Telecommunications Research Institute, 161 Kajong-Dong, Yusong-Gu, Taejon 305-350, Korea, Tel : 042-860-6738, Fax : 042-860-5199, e-mail : mutledosa@etri.re.kr

H. J. Eom is with the Department of Electrical Engineering, Korea Advanced Institute of Science and Technology, 373-1, Kusong Dong, Yusung Gu, Taejon, Korea, Tel . 042-869-3436, Fax · 042-869-8036, E-mail : hjeom@ec.kaist.ac.kr

Hankel functions of the first kind, respectively. $N_0(.)$ is the 0th order Neumann function. Note that ε_{ri} (i=1,2,3,4) are the relative permittivities of regions (I) through (IV).

In regions (II) and (III), the fields are represented as a summation of the discrete modes.

$$H_{\phi II}(\rho, z) = \sum_{m=0}^{\infty} \frac{i\omega\varepsilon_2}{k_{m2}} R_0'(k_{m2}\rho)\cos a_m(z+g) \qquad (3)$$

$$H_{\phi III}(\rho, z) = \sum_{m=0}^{\infty} \frac{-i\omega\varepsilon_3}{k_{\bar m3}} r_{\bar m} J_1(k_{\bar m3}\rho)\cos b_{\bar m}(z-t) \qquad (4)$$

where $R_0(k_{m2}\rho) = p_m \dfrac{H_0^{(1)}(k_{m2}\rho)}{H_1^{(1)}(k_{m2}b)} + q_m \dfrac{H_0^{(2)}(k_{m2}\rho)}{H_1^{(1)}(k_{m2}c)}$,

$k_{m2} = \sqrt{k_2^2 - a_m^2}$, $a_m = m\pi/d$, $k_{\bar m3} = \sqrt{k_3^2 - b_{\bar m}^2}$, and $b_{\bar m} = \bar m\pi/L$. We use the Fourier transform and mode-matching technique[4] to enforce the boundary conditions on the field continuities. Performing similar procedures as used in [4] at $\rho = b$, we obtain the following simultaneous equations:

$$\sum_{m=0}^{\infty}\left[\frac{H_0^{(1)}(k_{m2}b)}{H_1^{(1)}(k_{m2}b)} I_{ms} + \frac{\varepsilon_{r2}}{\varepsilon_{r1}}\frac{d}{2}\frac{\alpha_m}{k_{m2}}\delta_{ms}\right]p_m + \sum_{m=0}^{\infty}\left[\frac{H_0^{(2)}(k_{m2}b)}{H_1^{(2)}(k_{m2}c)} I_{ms} + \frac{\varepsilon_{r2}}{\varepsilon_{r1}}\frac{d}{2}\frac{H_1^{(2)}(k_{m2}b)}{H_1^{(2)}(k_{m2}c)}\frac{\alpha_m}{k_{m2}}\delta_{ms}\right]\cdot q_m = \frac{2i}{k_1 b}A_s(k_1) \qquad (5)$$

where δ_{ms} is the Kronecker delta, α_m = 2 ($m=0$), 1 ($m=1, 2, \ldots$), and

$$I_{ms} = \frac{2}{\pi}\int_0^{\infty}\frac{R'(kb)}{kR(kb)}A_m(\zeta)A_s(\zeta)d\zeta \qquad (6)$$

$$A_m(\zeta) = \frac{1}{2}[G_m^1(\zeta) + G_m^1(-\zeta)] \qquad (7)$$

$$G_m^1(\zeta) = \frac{-i\zeta[1-(-1)^m e^{-i\zeta d}]}{\zeta^2 - a_m^2}e^{-i\zeta g} \qquad (8)$$

In the same manner by applying the boundary conditions at $\rho = c$, we get

$$\sum_{m=0}^{\infty}\left[\frac{H_0^{(1)}(k_{m2}c)}{H_1^{(1)}(k_{m2}b)} J_{ms}^{00} - \frac{\varepsilon_{r2}}{\varepsilon_{r4}}\frac{d}{2}\frac{H_1^{(1)}(k_{m2}c)}{H_1^{(1)}(k_{m2}b)}\frac{\alpha_m}{k_{m2}}\delta_{ms}\right]p_m + \sum_{m=0}^{\infty}\left[\frac{H_0^{(2)}(k_{m2}c)}{H_1^{(2)}(k_{m2}c)} J_{ms}^{00} - \frac{\varepsilon_{r2}}{\varepsilon_{r4}}\frac{d}{2}\frac{\alpha_m}{k_{m2}}\delta_{ms}\right]q_m + \sum_{m=0}^{\infty} k_{\bar m}J_0(k_{\bar m3}c)J_{ms}^{10} = 0 \qquad (9)$$

$$\sum_{m=0}^{\infty}\left[\frac{H_0^{(1)}(k_{m2}c)}{H_1^{(1)}(k_{m2}b)} J_{m\bar s}^{00} p_m\right] + \sum_{m=0}^{\infty}\left[\frac{H_0^{(2)}(k_{m2}c)}{H_1^{(2)}(k_{m2}c)} J_{m\bar s}^{01} q_m\right] + \sum_{m=0}^{\infty}\left[J_0(k_{\bar m3}c)J_{\bar m\bar s}^{11} - \frac{\varepsilon_{r3}}{\varepsilon_{r4}}\frac{L}{2}J_1(k_{\bar m3}c)\frac{\alpha_{\bar m}}{k_{\bar m3}}\delta_{\bar m\bar s}\right]r_{\bar m} = 0 \qquad (10)$$

where

$$J_{ms}^{00} = \frac{1}{2\pi}\int_{-\infty}^{\infty}\frac{H_1^{(1)}(vc)}{vH_0^{(1)}(vc)}G_m^1(\zeta)G_s^1(-\zeta)d\zeta \qquad (11)$$

$$J_{\bar m s}^{10} = \frac{1}{2\pi}\int_{-\infty}^{\infty}\frac{H_1^{(1)}(vc)}{vH_0^{(1)}(vc)}G_{\bar m}^2(\zeta)G_s^1(-\zeta)d\zeta \qquad (12)$$

$$J_{m\bar s}^{01} = \frac{1}{2\pi}\int_{-\infty}^{\infty}\frac{H_1^{(1)}(vc)}{vH_0^{(1)}(vc)}G_m^1(\zeta)G_{\bar s}^2(-\zeta)d\zeta \qquad (13)$$

$$J_{\bar m\bar s}^{11} = \frac{1}{2\pi}\int_{-\infty}^{\infty}\frac{H_1^{(1)}(vc)}{vH_0^{(1)}(vc)}G_{\bar m}^2(\zeta)G_{\bar s}^2(-\zeta)d\zeta \qquad (14)$$

$$G_{\bar m}^2(\zeta) = \frac{-i\zeta[(-1)^{\bar m}e^{i\zeta L} - 1]}{\zeta^2 - b_{\bar m}^2}e^{i\zeta t} \qquad (15)$$

It is necessary to numerically integrate (11) through (14) using residue calculus or some other numerically efficient scheme. The input impedance at $z = -(d+g)$ is related to the reflection coefficient Γ_{in} by

$$Z_{in} = Z_c\frac{1+\Gamma_{in}}{1-\Gamma_{in}} \qquad (16)$$

$$\Gamma_{in} = \left.\frac{E_{\rho I}(\rho, z)}{E_{\rho I}^i(\rho, z)}\right|_{z=-(d+g)} = -[1+L_0(k_1)]e^{2ik_1(d+g)} \qquad (17)$$

$$L_0(k_1) = \sum_{m=0}^{\infty}\frac{k_1 R_o(k_{m2}b)}{\ln(b/a)(k_1^2 - a_m^2)}\cdot[(-1)^m\sin k_1(d+g) - \sin(k_1 g)] \qquad (18)$$

where $Z_c = \sqrt{\mu_0/\varepsilon_1}\, ln\left(\frac{b}{a}\right)/(2\pi)$ is the characteristic impedance of the input coaxial line. It is possible to evaluate the

Table 1. Comparison of our theory with [4]. (a=0.064 cm, b=0.2453 cm, c=3.81 cm, d=0.3175 cm, $\varepsilon_{r1} = \varepsilon_{r2}$ = 2.6, $\varepsilon_{r3} = \varepsilon_{r4}$ =1.0, $g = t = 0.0$, L = 0.01cm)

Frequency [GHz]	Predicted [4] (Γ_{in})	Our theory (Γ_{in})
1.0	−0.91571 − i 0.36941	−0.91586 − i 0.36939
1.5	−0.72116 − i 0.67392	−0.72128 − i 0.67396
3.0	0.29018 + i 0.50173	0.29019 + i 0.50176
4.0	−0.20957 − i 0.91768	−0.2091 − i 0.91694

Table 2. Convergence behavior as a function of L(a = 0.255 mm, $b = c$ = 0.84 mm, d = 2.0 mm, $\varepsilon_{r1} = \varepsilon_{r2}$ = 2.04, $\varepsilon_{r3} = \varepsilon_{r4}$ = 47 + i15.9211, $g = t$ = 0.0, f = 2.45 GHz, and mode number in region (II)=3)

L [cm]	Mode No. in region(III)	Input Impedance (Z_{in})	Reflection Coeff.
1.0	3	10.8372 + i 20.2795	−0.4793 − i 0.4931
	7	10.6784 + i 20.4507	−0.4799 − i 0.4987
	10	10.637 + i 20.4809	−0.4803 − i 0.4999
5.0	10	10.9409 + i 20.2235	−0.4781 − i 0.4905
	15	10.8694 + i 20.3684	−0.4774 − i 0.4943
	20	10.8132 + i 20.4409	−0.4774 − i 0.4966
	30	10.7447 + i 20.5097	−0.4777 − i 0.4989
10.0	20	10.9376 + i 20.2334	−0.4780 − i 0.4907
	30	10.866 + i 20.373	−0.4774 − i 0.4945
	40	10.8109 + i 20.4434	−0.4774 − i 0.4966

field distribution near the radiation slot by using Eqs. (2) and (3). To validate our theory, our results Γ_m in a limiting case $L \rightarrow 0$ are compared with [4], thus confirming an excellent agreement as shown in Table 1. In Table 2, we illustrate the convergence rate of our series solution for various L. The values for ε_{r3} and ε_{r4} correspond to the relative permittivities of conductive media - phantom simulating muscle tissues. When $L=1$, the input impedances for mode (m) numbers 3, 7, and 10 are similar each other. This means that our series solution is seen to converge rapidly. Since the numerical results for $L=1$ and 10 are almost identical, the effect of the hypothetical semi-infinite circular cylinder may be considered negligibly small.

Ⅲ. CONCLUSION

A simple analytic series solution for the radiation from a thermic endfire interstitial applicator is obtained using the Fourier transform. A hypothetical semi-infinite circular cylinder, which is added near the applicator, allows us to obtain the rigorous series solution. Numerical computations are performed to confirm the validity of our theoretical approach based on the Fourier transform and mode matching.

REFERENCES

[1] G. Cerri, R. D. Leo, and V. M. Primiani, "Thermic end-fire interstitial applicator for microwave hyperthermia", *IEEE Trans. Microwave Theory Tech.*, vol. 41, no. 6/7, pp. 1135-1142, June/July, 1993.

[2] M. S. Wu, L. Hamada, K. Ito, and H. Kasai, "Effect of a catheter on SAR distribution around interstitial antenna for microwave hyperthermia", *IEICE Trans. Commun.*, vol. E78-B, no. 6, pp. 845-850, June, 1995.

[3] A. D. Wunsch, "Effective impedance of a load filling a circumferential slot in a coaxial transmission line", *IEEE Trans. Microwave Theory Tech.*, vol. 35, no. 9, pp. 862-865, Sept., 1987.

[4] J. K. Park and H. J. Eom, "Fourier transform analysis of dielectric-filled edge-slot antenna", *Radio Sci.*, vol. 32, no. 6, pp. 2149-2154, Nov./Dec., 1997, Correction to Fourier transform analysis of dielectric-filled edge-slot antenna, vol. 33, no. 3, May-June, 1998.

Jong-Kweon Park

was born in Korea in 1969. He received the B.S. degree in electronic engineering from Kyungpook National University, Taegu in 1994, and the M.S. and Ph.D. degrees in electrical engineering from the Korea Advanced Institute of Science and Technology, Taejon in 1997 and 2001, respectively. He is now with the Antenna Technology Center, ETRI, Taejon. His research interests include wave scattering and antenna.

Hyo-Joon Eom

received the B.S. degree in electronic engineering from Seoul National University, Seoul and the M.S. and Ph.D. degrees in electrical engineering from the University of Kansas, Lawrence, Kansas, USA in 1977 and 1982, respectively. From 1981 to 1984, he was a Research Associate at the Remote Sensing Laboratory of the University of Kansas. From 1984 to 1989, he was with the Faculty of the Department of Electrical Engineering and Computer Science, University of Illinois, Chicago, Illinois USA. In 1989, he joined the Department of Electrical Engineering, Korea Advanced Institute of Science and Technology, Taejon, where he is now a Professor. His research interests include theoretical investigation on wave scattering and antenna.